Epitaxial Growth of Few-Layer Black Phosphorene Quantum Dots on Si Substrates

Hao Xu*, Xiaoyu Han*, Zhuangnan Li, Wei Liu, Xiao Li, Jiang Wu*, Zhengxiao Guo, Huiyun Liu

H. Xu, W. Liu, X. Li, Dr. J. Wu, Prof. H. Liu
Department of Electronic and Electrical Engineering, University College London
Torrington Place, London WC1E 7JE, United Kingdom
E-mail: hao.xu.15@ucl.ac.uk and jiang.wu@ucl.ac.uk
Dr. X. Han, Z. Li, Prof. Z. Guo
Department of Chemistry, University College London
20 Gordon St, Bloomsbury, London WC1H 0AJ, United Kingdom
E-mail: x.han@ucl.ac.uk
W. Liu
London Centre for Nanotechnology, University College London
London WC1H 0AH, United Kingdom

Elemental two-dimensional materials, such as silicene, germanene and stanene, have been synthesized by molecular beam epitaxy (MBE). However, the epitaxial growth of black phosphorene has been challenging to date. Herein, we report the successful MBE growth of few-layer black phosphorene quantum dots (BPQDs) directly on Si substrates at relatively low temperature using white phosphorus as the precursor. The formation of black phosphorene, was confirmed by atomic force microscopy, X-ray photoelectron spectroscopy and Raman spectroscopy, in combination with density functional theory (DFT) calculations. Uniform and pyramid-shaped BPQDs with an average radius of 27.5 ± 5 nm and height of 3.1 ± 0.6 nm were obtained at surface steps on fully deoxidized Si(111) substrates. The growth mechanism was probed by DFT at atomic level, demonstrating the crystallization of BPQDs at steps in preference to terraces on Si substrates of (111) and (100) surfaces. Our results show that BPQDs follow the Frank-van der Merwe growth mode and the favored few-layer growth trend with pyramid configuration. The realization of MBE-grown BPQDs enables the

1

synthesis of inch-sized low-dimensional black phosphorus with high purity and crystallinity, particularly promising for nanoelectronics and optoelectronics.

Two-dimensional (2D) materials harbour new and unique properties, compared with their 3D counterparts, and related research activities have escalated considerably in recent years.[1][2][3] Led by graphene in 2004,[4] materials in the 2D family have been extensively developed, including transition metal dichalcogenides (TMDs),[5] hexagonal boron nitride (h-BN),[6] MXenes,[7] black phosphorene (BP),[8][9] antimonene,[10,11] and tellurene,[12] *etc*. Each invokes different synthesis methods pertaining to their intrinsic structures and properties. Nonetheless, for further practical applications, such as sensors, transistors, lasers and energy storage, the success of each of those "enchanted" materials depends on the development of quality-controlled, efficient and scalable fabrication methods. Epitaxial growth, e.g. by chemical vapour deposition (CVD) or molecular beam epitaxy (MBE), has been widely used for 2D material synthesis, including graphene, silicene, germanene and MoS_2.[13][14][15][16]

BP nanosheets, as a relatively new member of the 2D family since 2014, have risen to the scientific limelight since its first fabrication by exfoliation.[8][9] BP possesses intriguing properties, such as bandgap tunability by layer thickness, doping and strain, *etc*.; in-plane anisotropy, particularly anisotropy in electron conductance; and high carrier mobility.[17][18] However, the fabrication of BP is still limited to poorly controlled mechanical and liquid exfoliations[19][20][21][22][23] and phase transition under harsh conditions[24][25]. Blue phosphorene, another allotrope of BP, has been fabricated using the MBE method. [26][27] There is no report on the synthesis of BP using a bottom-up method, to the best of our knowledge. Particularly, considerable efforts are needed to understand the formation mechanism of the BP, and its stability and sensitivity to substrate for continuous growth.

For the first time, we demonstrate the synthesis of black phosphorene quantum dots (BPQDs), as an attempt for above mentioned challenges, i.e. phase transition under the harsh conditions, of epitaxial growth of 2D BP, from white phosphorus directly on 3-inch Si substrates by MBE. Epitaxial BPQDs were grown on fully deoxidized Si(111) at 20 °C and Si(100) covered with native oxide at 15 °C, respectively. The as-grown BPQDs were characterized by atomic force microscopy (AFM), X-ray photoelectron spectroscopy (XPS), and Raman spectroscopy with BP fingerprint peaks. Uniform and pyramid-shaped BPQDs were obtained on Si(111) substrates, with an average radius of 27.5 ± 5 nm and height of 3.1 ± 0.6 nm. According to the AFM images, BPQDs preferably crystallized at the steps on the Si(111) surface. Comparatively, BPQDs on the non-deoxidized Si(100) substrate without observable surface steps, a rare case, were more intense and randomly distributed, and their radius was mainly between 8 and 14 nm and height between 1 and 2 nm. It should also be noted that BPQDs were rarely observed on Si substrates covered with native oxides. The distinct morphology of BPQDs observed on Si(100) not only indicates surface steps play a critical role in BP nucleation but also suggests surface orientation has a minor effect on the growth of BPQDs. DFT calculations reveal that the Si surface steps play an essential role both thermodynamically and kinetically for the epitaxial growth of BPQDs. Few-layer QD islands formed with a pyramid configuration were also demonstrated. The collective results show that BPQDs at the Si surface steps follow the Frank-van der Merwe growth mode. Additionally, the degradation of the BPQDs stored for 6-month was also studied. The current work provides a feasible means for synthesizing BP from common P allotropes, e.g. white phosphorus, in standard epitaxy systems. Therefore, BP can be synthesized in a large scale and integrated with materials into functional heterostructures. Our study enriches synthesis methods for BP other than exfoliation methods, and provides an insight of the epitaxial growth of BPQDs and guidance for further fabrication of two-dimensional BP nanosheets, nanoribbons or nanowires.

All samples were grown in an ultra-high vacuum MBE system in contrast to the conventional methods carried in high pressure and high temperature environment. Prior to deposition, the wafers were thermally outgassed at 600 °C for 1 hour. Both Si(111) and Si(100) wafers were used as the deposition substrates. The Si(111) wafer was heated to over 950 °C for 30 min to fully desorb the native oxide and then cooled to 20 °C, recorded by a thermal couple. After outgassing, the Si(100) wafer was transferred to the growth chamber and used as is. White phosphorus was evaporated from a valved cracker cell. The molecules were cracked in a high temperature cracking zone (900 °C). The beam flux was about 1×10^{-6} torr measured by a beam flux monitor. The deposition was carried out for about 20 min to form BPQDs as shown in **Figure 1**(a). After deposition, the samples were directly transferred out from the system for post-growth characterization.

Due to the propensity for degradation of the black phosphorene,[20][28] AFM was employed to characterize the surface morphology of the as-grown BPQDs/Si soon after the samples were taken out of the growth chamber. **Figure 2a** shows the natural steps and terraces on the (111)-oriented Si substrate after full deoxidization and the topography of BPQDs. Apparently, BPQDs preferred nucleating at the steps to terraces. This heterogeneous nucleation on surface steps was also reported for the self-assembly of InAs QDs on GaAs substrates, and associated with the naturally reconstructed surface on Si(111) substrates.[29] On the basis of the capillarity theory of nucleation, the step edges provided attachment sites of P adatoms by reducing the surface energy of clusters, with the possibility of guiding the nucleation in the process of compressively strained heteroepitaxy when forming arrays of QDs. In comparison, **Figure 3a** shows the AFM image of BPQDs grown on the (100)-oriented Si substrate with native oxide. As can be seen, more intense and randomly distributed BPQDs were observed. Further experimental discussions on the BPQDs/Si only focused on the (111) substrate unless state otherwise.

4

Density Functional Theory (DFT) calculations were carried out to provide a further insight in the MBE growth mechanism of the layered BPQDs on Si substrates. Firstly, the thermodynamic and kinetic interactions of cracked P_4 molecules from the white phosphorous with the Si(100) and (111) surfaces were studied. The Si(100)-4 × 2 and Si(111)-1 × 1 surfaces with single atomic steps were adopted for the study of the P_4 molecule adsorption on the stepped Si surfaces, as illustrated in Figures 1b, 1d and S1, respectively. The detailed computational settings and the surface analysis were listed in the experimental section. Four different adsorption sites on the Si(100) surface, including terrace dimer top (A), terrace hollow (B), step dimer top (C) and step hollow (D) were considered, as denoted in Figure 1b. Whereas for the Si(111) surface, two adsorption sites, terrace (E) and step position (F) (Figure 1d), were studied. The binding energy was calculated by $E_b = E_t - E_{P_4} - E_{sub}$, where E_t, E_{P4} and E_{sub} is the energy of total systems, P_4 molecule and Si substrates, respectively, and the results are listed in **Table 1**. For the Si(100) surface, the adsorption of P_4 molecule on the step sites (C and D) is exothermic whereas on the surface sites (A and B) is endothermic. Hence, it only should be expected the P_4 molecule could be found at the step sites of the Si (100) surface. Interestingly, the tetrahedron P_4 molecule unfolded into a chain on the silicon substrate at C site (Figure 1c), due to the bonding with both upper terrace dimer and lower terrace dimer Si atoms. The average bond length and angle of the buckled structure are 2.203 Å and 92.2°, respectively, compared with 2.22 Å and 95.8° in BP.[30] Collectively with the binding energy of the P_4 at C site, it suggests the new bonding of the P atoms with the substrate compensates the structure distortion of the P_4 molecule. For the Si(111) surface, the active Si(111) energetically provides a deposition bed at both terraces and steps (Table 1). Similarly to the Si(100), the tetrahedron P_4 molecule reformed to the buckled structure (see Figure 1e) with an average bond length of 2.239 Å. The strong chemical bonds were formed

with the binding energy of -3.179 eV at the step F site due to additional chemical bonds with Si atoms in the upper terrace besides those on the terraces. Further *ab*-initio Molecular Dynamics (AIMD) calculations show that these additional bonds could further help the P atoms diffusion along the steps (**Movie S1**). Within 5 ps at 300 K, the P atoms further dissolved and migrated along the steps. Though the terraces exothermically adsorbed the P_4 clusters, no major structure transformation occurred. Hence, the steps of the Si surfaces play an essential role as a seeding bed in further growth of BPQDs.

To prove the successful synthesis of BPQDs using the MBE method, XPS measurement was performed to determine the elemental composition of BPQDs/Si. In **Figure 4a**, the XPS spectrum of BPQDs/Si(111) with approximate 1 day ambient exposure (see black squares) exhibits spin-orbit split doublets of $2p_{3/2}$ and $2p_{1/2}$ at 129.4 eV and 130.5 eV, respectively, corresponding to the characteristics of crystallized BP.[31][32] A broad peak at 133.8 eV emerged and was assigned to phosphate species (PO_x) from oxidation when BPQDs exposed to ambient conditions.[33] Furthermore, a Raman spectrometer (see Figure 4b) was adopted to find the fingerprint vibration modes of BPQDs against the strong background signal from the Si substrate.[34] Notably, the 3-inch monocrystalline silicon substrate has high Raman cross-sections, while BPQDs have low optical absorption.[35][36] In spite of this, three peaks could be clearly observed at 366, 436 and 463 cm^{-1}, and can be assigned to one out-of-plane phonon mode (A_g^1) and two in-plane modes (B_{2g} and A_g^2), respectively, confirming the introduction of BPQDs onto the Si substrate.[19][37]

Further, the surface morphology was studied using statistical AFM analysis (see Figure 2b and 2c), revealing BPQDs had an average radius of 27.5 ± 5 nm and height of 3.1 ± 0.6 nm. Cross-sectional profiles along line 1 and 2 are shown in Figure 2d, respectively, in which the

thickness and pyramid shape of BPQDs, and Si surface step height were illustrated. According to the statistical AFM analysis (see Figure 3b and 3c), the radius of BPQDs/Si (100) was mainly around 8 to 10 nm, while the height 1 to 1.5 nm. Figure 3d shows the measured height along line 1 and 2, respectively. It could be concluded that the growth of BPQDs follows the Frank-van der Merwe mode on Si surfaces.

This Frank-van der Merwe growth mode of BPQDs was further studied by DFT calculations. Owning to the crystal structure of BP, there are three different edges, namely armchair (a), zig-zag (z) and diagonal (d) configurations.[30] We denoted those rhombus dots with diagonal terminations as the d-d dots (**Figure 5a – 5c**) and those rectangular dots with armchair and zigzag edges as the a-z dots (Figure 5d – 5f). The edge formation energy of the BPQDs was calculated based on the following equation:

$$E_f = (E_{total} - nE_P - mE_H)/L$$

Here, E_{total} is the total energy of the system, and E_P is the chemical energy of phosphorous and hydrogen, derived from the atoms in the BP and H_2 form, respectively. Additionally, n and m are the number of P and H atoms in the systems, respectively, and L is the perimeter of the dots. The results, listed in Table S1, show that the formation of dots with both edge configurations is energetically likely, and dots in a the larger size is more preferable, arising from the quantum confinement effect. However, the energy is not linearly decreasing, indicating the dots would reach to the energetically favoured size. When the dots stacked together, the layer stacking energy was defined as:

$$E_s = (E_{total} - \sum E_{dots})/x$$

Here, E_{total} and E_{dots} represent the total energy of the stacked BPQDs and the energy of each BPQD individually, respectively, and x is the number of overlapped atoms when dots stacking together. As shown in Figure 4c, **Table 2 and 3Error! Reference source not found.**, the

stacking energy of different combinations was calculated. When three 3×3 dots (Figure 5a and 5d) stack together, denoted as 3|3|3 and similarly for those 2|2|2 and 1|1|1, the stacking dots form in an orthorhombic shape. For a pyramid shape stacking, the 3×3, 2×2, and 1×1 dots stack in a 3|2|1 way. The others like 3|2|2, 3|1|1 and 2|1|1 are a rivet shape. Our results show that the d-d dots are keen on forming in an orthorhombic arrangement with only 39 meV energetically more favourable than the pyramid arrangement. Considering the thermodynamic entropy at room temperature, this energy difference could be neglected. For the a-z dots, they favour the pyramid shape stacking, which is consistent with the experimental results shown in Figure 2d and 3d. It should be also noted that the BPQDs with termination is essential as free-standing BPQDs are keen to clap into clusters, shown in **Figure S4**. Hence, the steps on the Si surface are crucial for the growth as they not only provide the seeding beds for the epitaxial growth of BPQDs but also stabilize the BPQDs.

After 6-month ambient exposure, only the peak corresponding to PO_x in XPS can be observed, while the eigen-peaks of BP disappeared, as shown by the magenta curve in Figure 4a. It is due to photo-induced oxidation and a layer-by-layer etching process of BPQDs after a long time exposure to ambient conditions.[38][28] This degradation behaviour in ambient conditions was also resolved in AFM images that displayed large bubble-like clusters on the substrates, as comparatively shown in **Figures S2 and S3**.

In summary, few-layer BPQDs were successfully fabricated directly on Si substrates using the MBE approach with cracked white phosphorus as the precursor. The formation of BP was confirmed by material characterizations of AFM, XPS and Raman spectroscopy, in combination with DFT calculations. Uniform and pyramid-shaped BPQDs on Si(111) were obtained at both the surface steps and terraces on the substrate surface, while the former was revealed as preferred sites. The BPQDs follow the Frank-van der Merwe growth mode on the

steps of the Si substrates. Theoretical calculation reveals that the surface steps of the Si provide not only the adsorption sites for P_4 molecules but also stabilize the BPQDs. Interestingly, we have observed that the BPQDs are prone to grow into a pyramid shape, as this configuration is characterised by a relatively low stacking energy.

Experimental Section

Molecular beam epitaxy: The samples were grown by a Veeco Gen930 Molecular Beam Epitaxy system. All the substrates were commercially available silicon wafers. The wafers are thermally outgassed at 600 °C for 1 hour in an ultrahigh vacuum preparation chamber before being transferred to an ultrahigh vacuum growth chamber equipped with a valved cracker P cell. Surface native oxide desorption was carried out for the Si(111) wafers by heating to over 950 °C for 30 min. The deposition of BPQDs was carried out at a substrate temperature from 15 to 20 °C, recorded by a thermal couple. White phosphorus was supplied to the Si surface by opening the cell valve and shutter. The phosphorus molecules were cracked in a high temperature cracking zone (900 °C). The deposition time of BP was about 20 min and the beam flux during deposition was about 1×10^{-6} torr measured by a beam flux monitor. Reflection high-energy electron diffraction (RHEED) was used for real-time in situ surface monitoring of BPQD growth (**Figure S5**).

Materials characterizations: AFM measurements were carried out in Veeco Dimension V Scanning Probe Microscope with tapping mode in the air. XPS measurements were performed in a Thermo Scientific system with an Al-Kα source. Raman spectroscopy was performed in a Renishaw inVia micro-Raman system using a 532 nm excitation laser and 1800 g mm^{-2} grating through a ×50 objective lens. The laser power was controlled at about 0.1 mW to avoid local heating effect.

Calculation details: All the calculations were carried out based on Density Functional Theory (DFT), implanted in Vienna ab initio Package (VASP).[39] The Project Augmented Wave

(PAW) method[40] was used, with the plane-wave cutoff set to 500 eV. The exchange-correlation energy was interpreted by the Perdew-Burke-Ernzerhof (PBE) functional[41], which have been proven sufficiently enough to mimic black phosphorene.[30] The van der Waals correction was treated using the DFT-D2 method of Grimme.[42] All the systems were set in a 30×60×40 Å box and relaxed until all the forces were less than 0.01 eV/Å. Gamma-only K-point was set to sample for the nanoflakes and 5×5×1 K-points for the P_4 molecules on the Si substrate study.

For the silicon substrates, the lattice parameter is optimised to 5.431 Å, in good agreement with the experiment observation.[43] For Si(100) surface, four surface reconstructions were considered, 2× 1, 2×2, 4×2 and asymmetry 2×1, where 4×2 possessed the lowest energy per Si atom and was chosen as further studied substrate. From previous experiment observation, atomic step occurs on the Si(100) surface in single-height step fashion.[44] The height profile on our Si(111) surface in Figure 2 indicates single atom steps for the Si(111) surface as well. Hence, the models of the silicon substrate were built in this fashion, shown in **Figure S1**.

The ab-initio Molecular Dynamic calculations (AIMD) were performed at 300 K with the Nose-Hoover method and lasted for 5 ps with 1fs intervals for each ionic movement.

Supporting Information
Supporting Information is available from the Wiley Online Library or from the author.

References

[1] A. K. Geim, K. S. Novoselov, *Nat. Mater.* **2007**, *6*, 183.

[2] K. S. Novoselov, V. I. Fal'ko, L. Colombo, P. R. Gellert, M. G. Schwab, K. Kim, *Nature* **2012**, *490*, 192.

[3] A. Castellanos-Gomez, *Nat. Photonics* **2016**, *10*, 202.

[4] K. S. Novoselov, A. K. Geim, S. V. Morozov, D. Jiang, Y. Zhang, S. V. Dubonos, I. V. Grigorieva, A. a. Firsov, *Science (80-.).* **2004**.

[5] K. F. Mak, C. Lee, J. Hone, J. Shan, T. F. Heinz, *Phys. Rev. Lett.* **2010**, *105*, 136805.

[6] K. Watanabe, T. Taniguchi, H. Kanda, *Nat. Mater.* **2004**, *3*, 404.

[7] N. Michael, K. Murat, P. Volker, L. Jun, N. Junjie, H. Min, H. Lars, G. Yury, B. M. W., *Adv. Mater.* **2011**, *23*, 4248.

[8] L. Li, Y. Yu, G. J. Ye, Q. Ge, X. Ou, H. Wu, D. Feng, X. H. Chen, Y. Zhang, *Nat. Nanotechnol.* **2014**, *9*, 1.

[9] H. Liu, A. T. Neal, *ACS Nano* **2014**, *8*, 4033.

[10] M. Fortin-Deschênes, O. Waller, T. O. Menteş, A. Locatelli, S. Mukherjee, F. Genuzio, P. L. Levesque, A. Hébert, R. Martel, O. Moutanabbir, *Nano Lett.* **2017**, *17*, 4970.

[11] Y. Shao, Z.-L. Liu, C. Cheng, X. Wu, H. Liu, C. Liu, J.-O. Wang, S.-Y. Zhu, Y.-Q. Wang, D.-X. Shi, K. Ibrahim, J.-T. Sun, Y.-L. Wang, H.-J. Gao, *Nano Lett.* **2018**, *18*, 2133.

[12] Z. Zhu, X. Cai, S. Yi, J. Chen, Y. Dai, C. Niu, Z. Guo, M. Xie, F. Liu, J.-H. Cho, Y. Jia, Z. Zhang, *Phys. Rev. Lett.* **2017**, *119*, 106101.

[13] J. M. Garcia, U. Wurstbauer, A. Levy, L. N. Pfeiffer, A. Pinczuk, A. S. Plaut, L. Wang, C. R. Dean, R. Buizza, A. M. Van Der Zande, J. Hone, K. Watanabe, T. Taniguchi, *Solid State Commun.* **2012**, *152*, 975.

[14] M. Derivaz, D. Dentel, R. Stephan, M. C. Hanf, A. Mehdaoui, P. Sonnet, C. Pirri, *Nano Lett.* **2015**, *15*, 2510.

[15] P. Vogt, P. De Padova, C. Quaresima, J. Avila, E. Frantzeskakis, M. C. Asensio, A. Resta, B. Ealet, G. Le Lay, *Phys. Rev. Lett.* **2012**, *108*, 155501.

[16] E. G. Blackman, E. E. Mamajek, R. D. Cottrell, M. K. Watkeys, D. Bauch, J. W. Hernlund, N. Coltice, R. Magnetism, *Science (80-.).* **2015**, *349*, 524.

[17] M. Batmunkh, M. Bat-Erdene, J. G. Shapter, *Adv. Mater.* **2016**, *28*, 8586.

[18] A. Carvalho, M. Wang, X. Zhu, A. S. Rodin, H. Su, A. H. Castro Neto, *Nat. Rev. Mater.* **2016**, *1*, 16061.

[19] H. U. Lee, S. Y. Park, S. C. Lee, S. Choi, S. Seo, H. Kim, J. Won, K. Choi, K. S. Kang, H. G. Park, H. S. Kim, H. R. An, K. H. Jeong, Y. C. Lee, J. Lee, *Small* **2016**, *12*, 214.

[20] J. Shao, H. Xie, H. Huang, Z. Li, Z. Sun, Y. Xu, Q. Xiao, X.-F. Yu, Y. Zhao, H. Zhang, H. Wang, P. K. Chu, *Nat. Commun.* **2016**, *7*, 12967.

[21] Z. Sofer, D. Bouša, J. Luxa, V. Mazanek, M. Pumera, *Chem. Commun.* **2016**, *52*, 1563.

[22] X. Zhang, H. Xie, Z. Liu, C. Tan, Z. Luo, H. Li, J. Lin, L. Sun, W. Chen, Z. Xu, L. Xie, W. Huang, H. Zhang, *Angew. Chemie - Int. Ed.* **2015**, *54*, 3653.

[23] Z. Sun, H. Xie, S. Tang, X. F. Yu, Z. Guo, J. Shao, H. Zhang, H. Huang, H. Wang, P. K. Chu, *Angew. Chemie - Int. Ed.* **2015**, *54*, 11526.

[24] X. Li, B. Deng, X. Wang, S. Chen, M. Vaisman, S. Karato, G. Pan, M. Larry Lee, J. Cha, H. Wang, F. Xia, *2D Mater.* **2015**, *2*, 031002.

[25] J. B. Smith, D. Hagaman, H.-F. Ji, *Nanotechnology* **2016**, *27*, 215602.

[26] Z. Zhu, D. Tomanek, *Phys. Rev. Lett.* **2014**, *112*, 1.

[27] J. L. Zhang, S. Zhao, C. Han, Z. Wang, S. Zhong, S. Sun, R. Guo, X. Zhou, C. D. Gu, K. Di Yuan, Z. Li, W. Chen, *Nano Lett.* **2016**, *16*, 4903.

[28] A. Favron, E. Gaufrès, F. Fossard, A.-L. Phaneuf-L'Heureux, N. Y.-W. Tang, P. L. Lévesque, A. Loiseau, R. Leonelli, S. Francoeur, R. Martel, *Nat. Mater.* **2015**, *14*, 826.

[29] F. Patella, A. Sgarlata, F. Arciprete, S. Nufris, P. D. Szkutnik, E. Placidi, M. Fanfoni, N. Motta, A. Balzarotti, *J. Phys. Condens. Matter* **2004**, *16*, S1503.

[30] X. Han, H. Morgan Stewart, S. A. Shevlin, C. R. A. Catlow, Z. X. Guo, *Nano Lett.* **2014**, *14*, 4607.

[31] D. W. Bullett, *Solid State Commun.* **1985**, *55*, 257.

[32] A. H. Woomer, T. W. Farnsworth, J. Hu, R. A. Wells, C. L. Donley, S. C. Warren, *ACS Nano* **2015**, *9*, 8869.

[33] J. D. Wood, S. A. Wells, D. Jariwala, K. Chen, E. Cho, V. K. Sangwan, X. Liu, L. J. Lauhon, T. J. Marks, M. C. Hersam, *Nano Lett.* **2014**, *14*, 6964.

[34] M. Khorasaninejad, J. Walia, S. S. Saini, *Nanotechnology* **2012**, *23*, 275706.

[35] A. Hammouda, A. Canizarès, P. Simon, A. Boughalout, M. Kechouane, *Vib. Spectrosc.* **2012**, *62*, 217.

[36] A. Castellanos-gomez, L. Vicarelli, E. Prada, J. O. Island, K. L. Narasimha-Acharya, S. I. Blanter, D. J. Groenendijk, M. Buscema, G. A. Steele, J. V Alvarez, H. W. Zandbergen, J. J. Palacios, H. S. J. Van Der Zant, *2D Mater.* **2014**, *1*, 025001.

[37] V. Eswaraiah, Q. Zeng, Y. Long, Z. Liu, *Small* **2016**, *12*, 3480.

[38] J. O. Island, G. A. Steele, H. S. J. Van Der Zant, A. Castellanos-gomez, *2D Mater.* **2015**, *2*, 1.

[39] G. Kresse, D. Joubert, *Phys. Rev. B* **1999**, *59*, 1758.

[40] G. Kresse, J. Furthmüller, *Comput. Mater. Sci.* **1996**, *6*, 15.

[41] J. P. Perdew, K. Burke, M. Ernzerhof, *Phys. Rev. Lett.* **1996**, *77*, 3865.

[42] S. Grimme, *J. Comput. Chem.* **n.d.**, *27*, 1787.

[43] T. Hom, W. Kiszenik, B. Post, *J. Appl. Crystallogr.* **1975**, *8*, 457.

[44] J. A. Martin, C. E. Aumann, D. E. Savage, M. C. Tringides, M. G. Lagally, W. Moritz, F. Kretschmar, *J. Vac. Sci. Technol. A* **1987**, *5*, 615.
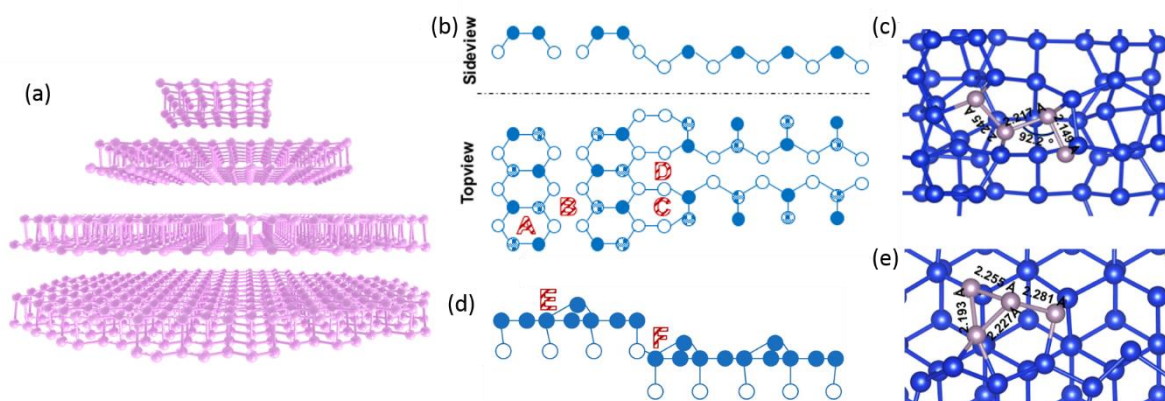
Figure 1. Schematics of a BPQD, and Si(100) and (111) surfaces. (a) The 3D schematic diagram of BPQD. (b, d) The schematics of the Si(100)-4×2 and Si(111)-1×1 surfaces in single atom height step, respectively. The solid circles and unfilled circles represent the first and second layer atoms, respectively. The solid and pattern filled circles represent the buckled up and down atoms in Si(100)-4×2. Four deposition positions for P_4 molecule on Si(100)-4×2 denoted A, B, C and D represent surface dimer top, surface hollow, step dimer top and step hollow, respectively. Two deposition position marked E and F represent P_4 molecules on the terrace and step of Si(111))-1×1 surface. (c, e) The desorbed P_4 molecule on Si(100) C site and Si(111) F site, respectively. Each bond length and bond angle were labeled. The blue and purple balls represent Si and P atoms, respectively.
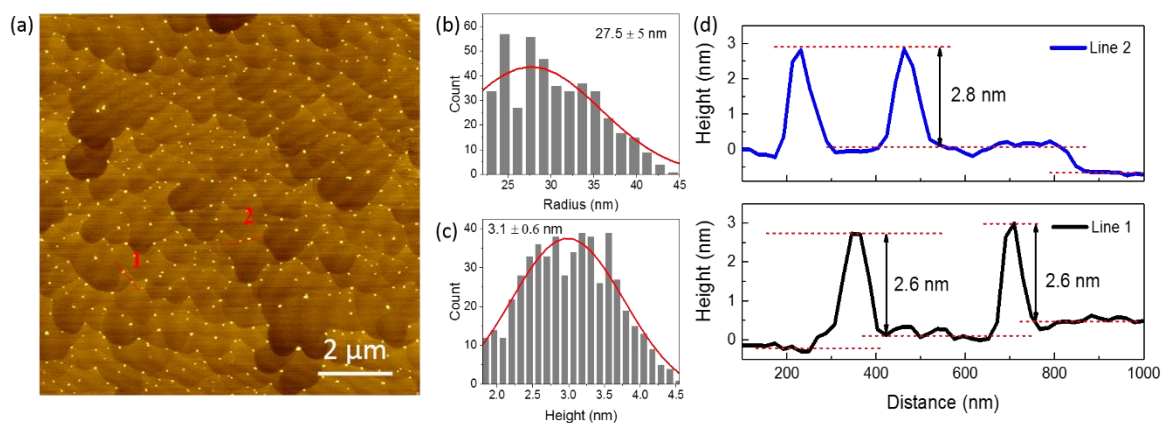
Figure 2. AFM results of BPQDs grown on Si(111). (a) AFM morphology. (b) Statistical distribution of size. (c) Statistical distribution of height. (d) Height profiles along line 1 and 2, respectively.
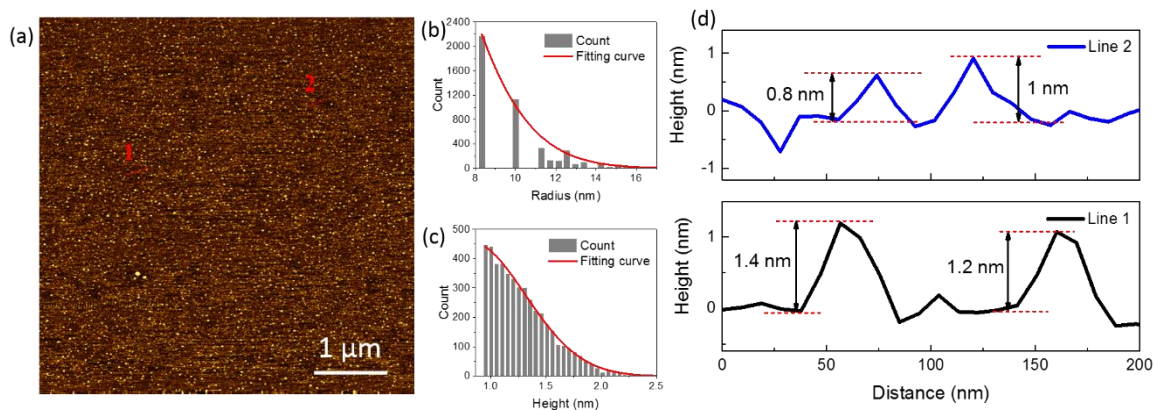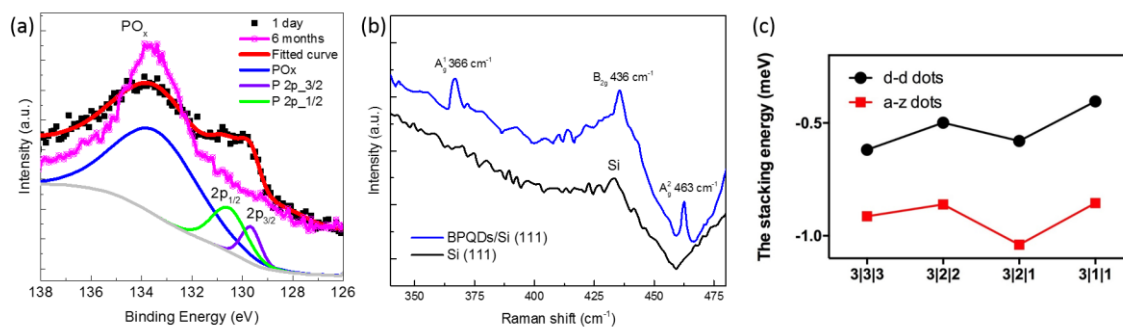
Figure 3. AFM results of BPQDs grown on Si(100). (a) AFM morphology. (b) Statistical distribution of size. (c) Statistical distribution of height. (d) Height profiles along line 1 and 2, respectively.

Figure 4. (a) XPS spectra of BPQDs/Si(111) with different ambient exposure time. (b) Raman spectra of BPQDs and Si substrate. (c) The stacking energy (meV) of three different size dots in different arrangement.
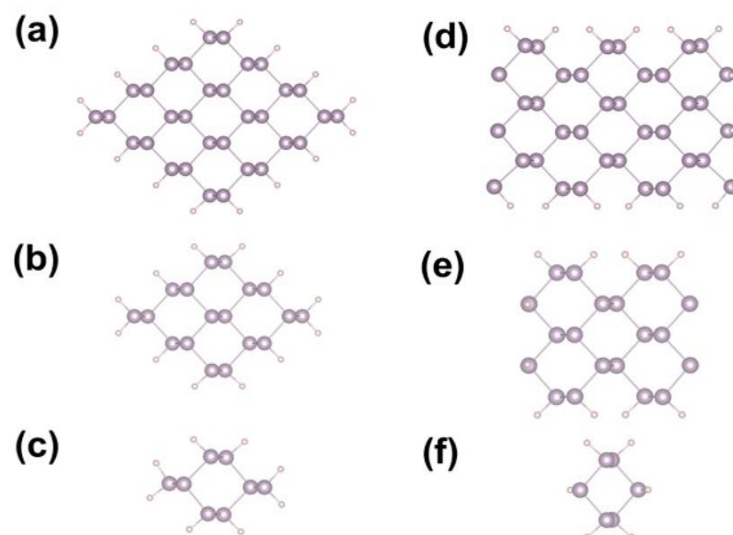
Figure 5. Three different sizes, 3×3, 2×2, 1×1 of the d-d BPQDs were shown in (a), (b), and (c), respectively, and three different sizes 3×3, 2×2, 1×1 of the a-z BPQDs were shown in (d), (e), and (f), respectively.

Table 1. Binding energy (eV) of the P_4 molecules on Si(100)-4 × 2 and Si(111)-1×1 surfaces. The denotation of the sites was shown in Figure 1b and 1d.

	Deposition position	E_b (eV)
Si(100)-4 × 2	A	0.166
	B	0.431
	C	-0.272
	D	-0.121
Si(111)-1×1	E	-0.738
	F	-3.179

Table 2. Stacking energy (meV) of different size combinations of d-d dots.

cylinder	3×3	2×2	1×1
Bilayer	-0.617	-0.382	-0.208
Trilayer	-0.619	-0.357	-0.217
pyramid	*3/2/2*	*3/2/1*	*3/1/1*
	-0.499	-0.580	-0.404

Table 3. Stacking energy (meV/atom) of different size combinations of a-z dots.

cylinder	3×3	2×2	1×1
Bilayer	-0.847	-0.639	-0.395
Trilayer	-0.914	-0.734	-0.329
pyramid	*3/2/2*	*3/2/1*	*3/1/1*
	-0.861	-1.04	-0.855

Pyramid-shaped black phosphorene quantum dots were obtained at surface steps of deoxidized Si(111) substrates by molecular beam epitaxy. The growth mechanism was probed by density function theory at atomic level, demonstrating the crystallization of black phosphorene quantum dots at steps, in preference to terraces on Si substrates.

Keywords: black phosphorene; quantum dots; molecular beam epitaxy; density functional theory

Hao Xu*, Xiaoyu Han*, Zhuangnan Li, Wei Liu, Xiao Li, Jiang Wu*, Zhengxiao Guo, Huiyun Liu

Epitaxial Growth of Few-Layer Black Phosphorene Quantum Dots on Si Substrates

ToC figure
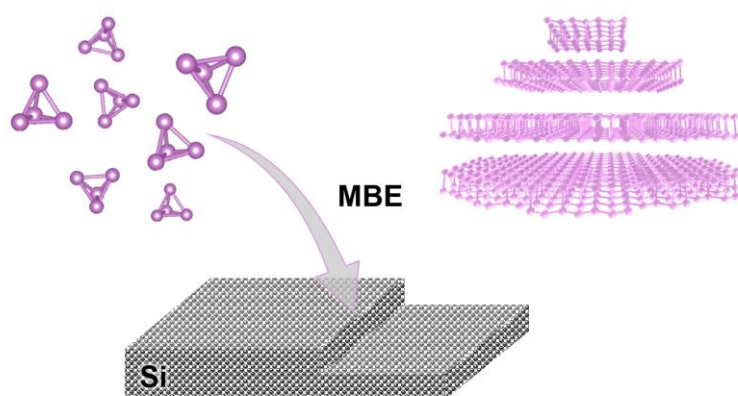
Supporting Information

Epitaxial Growth of Few-Layer Black Phosphorene Quantum Dots on Si Substrates

Hao Xu*, Xiaoyu Han*, Zhuangnan Li, Wei Liu, Xiao Li, Jiang Wu*, Zhengxiao Guo, Huiyun Liu
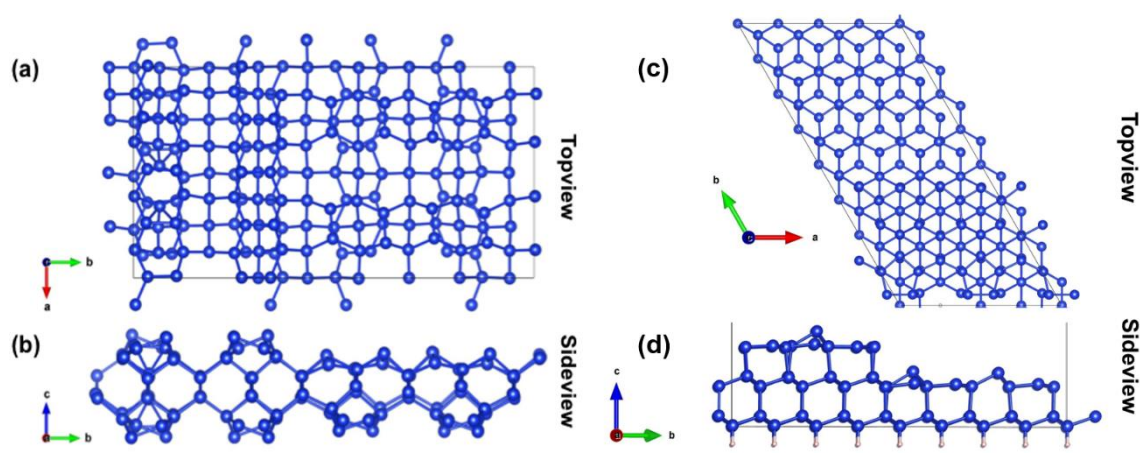

Figure S1. The top view (a) and side view (b) of Si(100)-4×2 slab in a single step. The top view (c) and side view (d) of Si(111)-1×1 slab in the single step.
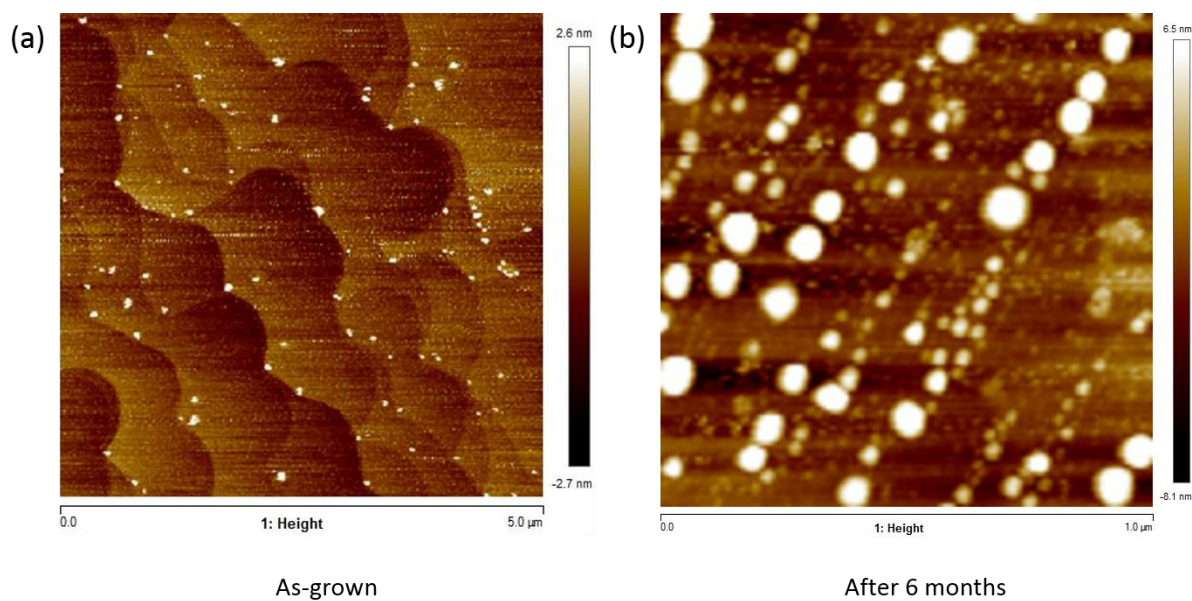
(a) As-grown

(b) After 6 months

Figure S2. AFM images of the as-grown (a) and ambient exposed for 6 months (b) of BPQDs/Si(111).
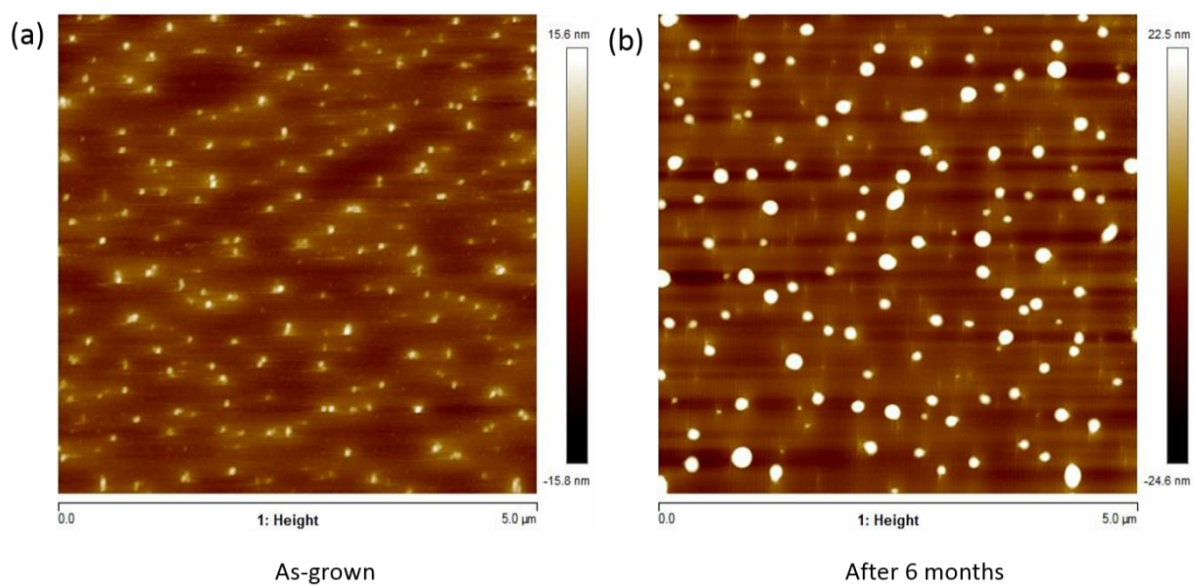
Figure S3. AFM images of the as-grown (a) and ambient exposed for 6 months (b) of BPQDs/Si(100).
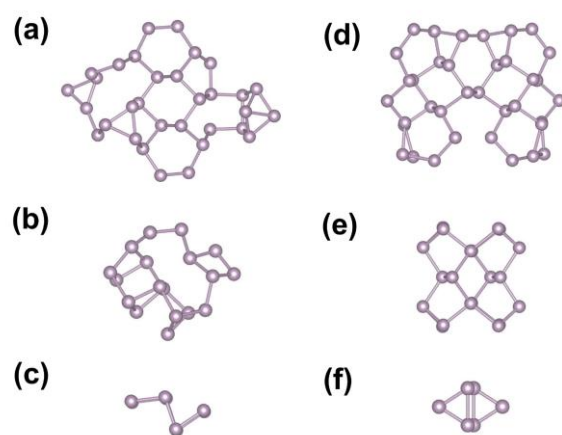
Figure S4. The different scale d-d and a-z dots without H termination, corresponding to those shown in Figure 5. They clapped into clusters without the surface step on the substrate.
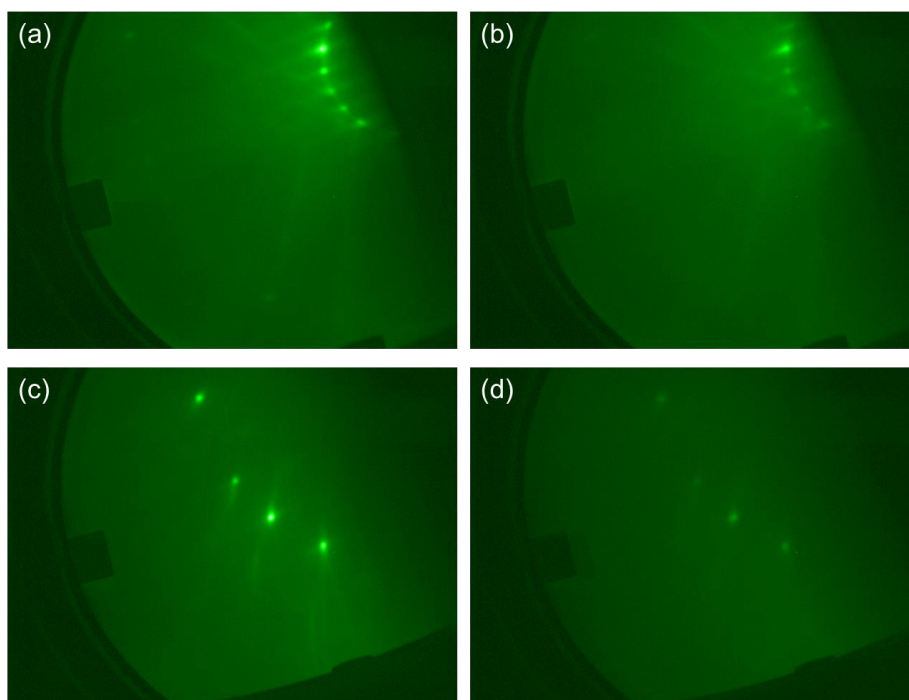
Figure S5. The RHEED patterns (a) before and (b) during deposition of P on the Si(100) surface and (c) before and (d) during deposition of P on the Si(111) surface.

Table S1. The edge formation energy (eV/ Å) of the different size (3×3, 2×2, and 1×1) of BPQDs.

	d-d dots	a-z dots
3×3	-0.311	-0.314
2×2	-0.276	-0.293
1×1	-0.186	-0.127